Aspalathin and Nothofagin from Rooibos (*Aspalathus linearis*) Inhibits High Glucose-Induced Inflammation *In Vitro* and *In Vivo*

Sae-Kwang Ku,[1] Soyoung Kwak,[2] Yaesol Kim,[2] and Jong-Sup Bae[2,3]

Abstract—Vascular inflammation plays a key role in the initiation and progression of atherosclerosis, a major complication of diabetes mellitus. Aspalathin (Asp) and nothofagin (Not) are two major active dihydrochalcones found in green rooibos, which have been reported for their antioxidant activity. In this study, we assessed whether Asp or Not can suppress vascular inflammation induced by high glucose (HG) in human umbilical vein endothelial cells (HUVECs) and mice. We monitored the effects of Asp or Not on HG-induced vascular hyperpermeability, expression of cell adhesion molecules (CAMs), formation of reactive oxygen species (ROS), and activation of nuclear factor (NF)-κB *in vitro* and *in vivo*. Our data indicate that HG markedly increased vascular permeability, monocyte adhesion, expression of CAMs, formation of ROS, and activation of NF-κB. Remarkably, treatment of Asp or Not inhibited HG-mediated vascular hyperpermeability, adhesion of monocytes toward HUVECs, and expression of CAMs. In addition, Asp or Not suppressed the formation of ROS and the activation of NF-κB. Since vascular inflammation induced by HG is critical in the development of diabetic complications, our results suggest that Asp or Not may have significant benefits in the treatment of diabetic complications.

KEY WORDS: aspalathin; nothofagin; high glucose; diabetes mellitus; inflammation.

INTRODUCTION

Diabetes mellitus is a metabolic disorder affecting carbohydrate, fat, and protein metabolism, and it represents a heterogeneous group of disorders having hyperglycemia, which is due to impaired glucose utilization resulting from a defective or deficient insulin secretory response [1, 2]. Along with hyperglycemia and abnormalities in serum lipids, diabetes is associated with microvascular and macrovascular complications which are the major causes of morbidity and death in diabetic subjects [1–3]. Diabetes is

a major public health issue that is rapidly getting worse, in part, due to its impact on adults of working age in developing countries [3]. Approximately 366 million people have diabetes, among which, 80 % resides in developing countries. Further, this number is expected to rise to 552 million by 2030 [1]. Although diabetes is generally not recorded as a cause of death, complications from diabetes are believed to be the fifth leading cause of death after communicable diseases, cardiovascular disease, cancer, and injuries [4].

Diabetes can be managed by regular exercise, diet, oral medication, or insulin. However, the available therapeutics are limited in their ability to treat diabetes mellitus due to a lack of systemic efficacy, issues with patient compliance, and adverse side effects [5]. As such, there has been a widespread effort to identify alternative therapies, such as effective hypoglycemic agents, for the treatment of diabetes mellitus. Recently, the World Health Organization (WHO) recommended evaluation of plants for the treatment of diseases that lack safe and effective therapeutics [6]. Management of diabetes without any side

Sae-Kwang Ku and Soyoung Kwak contributed equally to this work.

[1] Department of Anatomy and Histology, College of Korean Medicine, Daegu Haany University, Gyeongsan, 712-715, Republic of Korea
[2] College of Pharmacy, CMRI, Research Institute of Pharmaceutical Sciences, Kyungpook National University, 80 Dahak-ro, Buk-gu, Daegu, 702-701, Republic of Korea
[3] To whom correspondence should be addressed at College of Pharmacy, CMRI, Research Institute of Pharmaceutical Sciences, Kyungpook National University, 80 Dahak-ro, Buk-gu, Daegu, 702-701, Republic of Korea. E-mail: baejs@knu.ac.kr

effects is still a challenge to the medical system. This leads to increasing demand for natural products with antidiabetic activity and less side effects. Interestingly, many indigenous plants have been used to manage diabetes, and some of these plants have been tested and their active ingredients isolated [7].

Teas and herbal infusions are natural beverages which contain compounds that are of particular interest to the health sciences due to their potential *in vivo* biological properties [8, 9]. Infusions of the herbal tea rooibos (*Aspalathus linearis*, a plant endemic to the Western Cape Province of South Africa) are caffeine-free, low-tannin beverages that are a source of uncommon glycosylated polyphenol compounds [10]. It is known that abundant flavonoids are contained in Rooibos tea, particularly Asp and Not [11]. It has been reported that the antioxidant activity of natural rooibos infusions and extracts depends on the total polyphenol content of the sample, which is determined by how the plant is processed [10]. Rooibos tea contains sodium, potassium, magnesium, calcium, and trace elements such as zinc. Although some biological activities and pharmacological functions of Asp and Not have been reported, the effects of Asp and Not on high glucose (HG)-induced inflammatory responses have not been studied. In this study, we assessed the ability of Asp and Not to suppress vascular inflammation induced by HG in primary cultured human endothelial cells and mice.

MATERIALS AND METHODS

Reagents

Nothofagin was obtained from Chem Faces (Wuhan, China). Aspalathin, D-glucose, L-glucose, D-mannitol, Evans blue, 2-mercaptoethanol, and antibiotics (penicillin G and streptomycin) were purchased from Sigma (St. Louis, MO, USA). Fetal bovine serum (FBS) and Vybrant DiD were purchased from Invitrogen (Carlsbad, CA, USA).

Cell Culture

Primary human umbilical vein endothelial cells (HUVECs) were obtained from Cambrex Bio Science (Charles City, IA, USA) and maintained as described previously [12]. All experiments were carried out with HUVEC at passages 3–5. THP-1 cells, a monocyte cell line, were maintained as previously described [13].

Animals and Husbandry

Male C57BL/6 mice (6–7 weeks old; weight, 18–20 g) purchased from Orient Bio Co. (Sungnam, KyungKiDo, Republic of Korea) were used following a 12-day acclimatization period. All animals were treated in accordance with the Guidelines for the Care and Use of Laboratory Animals issued by Kyungpook National University (KNU2012-13).

Cell Viability Assay

MTT was used as an indicator of cell viability. Cells were grown in 96-well plates at a density of 5×10^3 cells/well. After 24 h, cells were washed with fresh medium, followed by treatment with the compounds. After incubating for 48 h, the cells were washed, and 100 μL of MTT (1 mg/mL) was added, followed by incubation for 4 h. Finally, DMSO (150 μL) was added to solubilize the formazan salt formed. The amount of formazan salt was determined by measuring the OD at 540 nm using a microplate reader (Tecan Austria GmbH, Austria).

Permeability Assay *In Vitro*

Endothelial cell permeability in response to increasing concentrations of each compound was quantified by spectrophotometric measurement of the flux of Evans blue-bound albumin across functional cell monolayers using a modified 2-compartment chamber model, as previously described [14]. HUVECs were plated (5×10^4 cells/well) in a 3-μm pore size and 12-mm diameter transwell for 3 days. Confluent monolayers were incubated with increasing concentrations of the compounds for 6 h, followed by incubation with the indicated concentrations of HG for 24 h. The assay was then performed as previously described [14].

Permeability Assays *In Vivo*

Mice were pretreated with intravenous administration of each compound. After 6 h, 1 % Evans blue dye solution in normal saline was administered by intravenous injection to each mouse, immediately followed by an intravenous injection of HG (9 mg/kg). Thirty minutes later, the mice were sacrificed. The peritoneal exudates were collected after being washed with 5 mL of normal saline and centrifuged at $200 \times g$ for 10 min. Vascular permeability was determined as previously described [15, 16].

Expression of CAMs

Expression of vascular cell adhesion molecule-1 (VCAM-1), intercellular adhesion molecule-1 (ICAM-1), and E-selectin was determined by whole-cell ELISA, as previously described [17, 18]. Briefly, HUVEC mono-layers were treated with the compounds at the indicated concentrations for 6 h, followed by treatment with HG (25 mM) for 24 h. Cells were fixed in 1 % paraformalde-hyde and washed three times. Mouse antihuman monoclo-nal antibodies (VCAM-1, ICAM-1, E-selectin, Temecula, CA, USA, 1:50 each) were added, and the cells were incubated for 1 h (37 °C, 5 % CO$_2$), followed by washing. Finally, cells were treated with peroxidase-conjugated anti-mouse IgG antibody (Sigma, St. Louis, MO) for 1 h, washed three times, and then developed using o-phenyl-enediamine substrate (Sigma, St. Louis, MO). All measure-ments were performed in triplicate wells.

Cell–Cell Adhesion Assay

Adherence of monocytes to endothelial cells was evaluated by fluorescent labeling of monocytes, as previ-ously described [17, 18]. Briefly, monocytes were labeled with 5 µM Vybrant DiD for 20 min at 37 °C in phenol red-free RPMI containing 5 % fetal bovine serum. After wash-ing, the cells (1.5×10^6 cells/mL, 200 µL/well) were resuspended in adhesion medium (RPMI containing 2 % fetal bovine serum and 20 mM HEPES). The cells were then added to confluent monolayers of HUVECs in 96-well plates. Prior to the addition of cells, HUVECs were treated 6 h with the compounds, followed by treatment with HG (25 mM for 24 h). Quantification of cell adhesion was determined as previously described [17, 18].

RNA Preparation and Real-Time qRT-PCR

HUVECs were grown in six-well plates and incubat-ed with each compound for 6 h, followed by HG (25 mM for 24 h). The High Pure RNA Isolation kit (Roche Diagnostics) was used for the isolation of RNA from cell culture. RNA quality was tested by measuring the ratio 260/280 nm in a UV–spectrophotometer. For each sample, 0.5 µg of total RNA was reverse transcribed into comple-mentary DNA (cDNA) using the Transcriptor First Strand cDNA Synthesis kit (Roche Diagnostics).

Real-time PCR analysis was performed using the LightCycler® 96 System (Roche Diagnostics, Mannheim, Germany) using FastStart Essential DNA Green Master (Roche Diagnostics) according to the manufacturer's instructions. Glyceraldehyde 3-phosphate dehydrogenase (GAPDH) was used as an internal control. The relative quantification of messenger RNA (mRNA) expression was calculated as the ratio of the target gene to GAPDH. Specific sense and antisense primers used were as follows: monocyte chemotactic protein (MCP)-1, sense: 5′-TGCA GAGGCTCGCGAGCTA-3′; antisense: 5′-CAGGTGGT CCATGGAATCCTGA-3′, interleukin (IL)-8, sense: 5′-ACTGAGAGTGATTGAGAGTGGAC-3′; antisense: 5′-AACCCTCTGCACCCAGTTTTC-3′, GAPDH, sense: 5′-GTCTTCACTACCATGGAGAAGG-3′; and antisense: 5′-TCATGGATGACCTTGGCCAG-3′.

Western Blotting

Confluent monolayers of HUVECs were treated with the compounds at the indicated concentrations for 6 h, followed by treatment with HG (25 mM) for 24 h. After the proteins were prepared by lysing the cells, equal amounts of protein were separated by SDS-PAGE (10 %) and electroblotted overnight onto Immobilon membranes (Millipore, Billerica, MA, USA). The membranes were blocked for 1 h with 5 % low-fat milk powder TBS (50 mM Tris–HCl, pH 7.5, 150 mM NaCl) containing 0.05 % Tween 20, followed by incubation with anti-MCP-1, anti-IL-8, and anti-GAPDH antibodies (Santa Cruz Biotechnology, Dallas, TX, USA) at room tempera-ture for 1.5 h; this was followed by incubation with horse-radish peroxidase-conjugated secondary antibody and ECL detection, according to the manufacturer's instructions.

H$_2$O$_2$ Release Assay

Extracellular production of H$_2$O$_2$ was quantified us-ing the Amplex Red Hydrogen Peroxide Assay Kit (Molecular Probes; Eugene, OR, USA), according to the manufacturer's recommendations. Cells were washed twice with ice-cold PBS, harvested by microcentrifugation, and resuspended in a Krebs-Ringer phosphate (KRPG) solution. The reaction mixture (100 µL, 50 µM Amplex Red reagent containing 0.1 U/mL HRP in KRPG) was added to each microplate well and then prewarmed at 37 °C for 10 min. The reaction was started by the addition of resuspended cells in 20 µL of KRPG. Fluorescence readings became stable within 30 min of starting the reac-tion equipped for absorbance at ~560 nm (Multiskan, Thermo Labsystems Inc., Franklin, MA, USA). A reagent H$_2$O$_2$ standard curve was used for the calculation of H$_2$O$_2$ concentration.

Preparation of Cytoplasmic and Nuclear Extracts

Cells were harvested rapidly by sedimentation, and the nuclear and cytoplasmic extracts were prepared on ice, as previously described [19]. Cells were harvested and washed with 1 mL buffer A (10 mM HEPES, pH 7.9, 1.5 mM MgCl$_2$, 19 mM KCl) for 5 min at 600 g. The cells were then resuspended in buffer A, centrifuged at 600g for 3 min, resuspended in 30 μL buffer B (20 mM HEPES, pH 7.9, 25 % glycerol, 0.42 M NaCl, 1.5 mM MgCl$_2$, 0.2 mM EDTA), rotated for 30 min at 4 °C, and then centrifuged at 13,000g for 20 min. The supernatant was used as the nuclear extract.

Immunofluorescence Staining

HUVECs were grown to confluence on glass cover slips coated with 0.05 % poly-L-lysine in complete media containing 10 % FBS and maintained for 48 h. Cells were stimulated with HG (25 mM) for 1 h, with or without prior treatment with the compounds for 2 h. After several washes with PBS, cells were fixed in 4 % formaldehyde in PBS (*v/v*) for 15 min at room temperature. For immunostaining, cells were permeabilized in 0.05 % Triton X-100 in PBS for 15 min and blocked in blocking buffer (5 % BSA in PBS) overnight at 4 °C. Cells were incubated with primary rabbit monoclonal NF-κB p65 antibody and anti-rabbit Alexa 488 overnight at 4 °C. Nuclei were counterstained with 4,6-diamidino-2-phenylindole dihydrochloride (DAPI). Cells were then visualized by confocal microscopy at ×63 magnification (TCS-Sp5, Leica Microsystems, Germany). Quantification of p65 nuclear translocation was calculated, as described previously [20, 21].

ELISA for NF-κB

Total and phosphorylated p65 NF-κB (#7174, #7173, Cell Signaling Technology, Danvers, MA, USA) in nuclear lysates was determined using ELISA kits. Values were measured using an ELISA plate reader (Tecan, Austria GmbH, Austria).

Statistical Analysis

All experiments were performed independently at least three times. Values are expressed as means±standard error of the mean (SEM). The statistical significance of differences between test groups was evaluated by one-way analysis of variance (ANOVA) Tukey's post-test (SPSS, version 14.0, SPSS Science, Chicago, Il, USA), and p values less than 0.05 ($p<0.05$) were considered significant.

RESULTS AND DISCUSSION

Aspalathin (Asp, 2′,3,4,4′,6′-pentahydroxy-3′-C-β-D-glucopyranosyldihydrochalcone) and nothofagin (Not, the 3-deoxy analogue of aspalathin) are compounds found in rooibos and aspalathin is unique to rooibos. The relatively large quantities of aspalathin present in the dried aerial parts of the rooibos plant (4.5–9.3 %) have led to the production of extracts from green rooibos for the food, beverage, and cosmetic industries [22]. Nothofagin is present in much lower quantities compared to aspalathin [22]. It is well known that HG-induced vascular inflammatory responses such as the upregulation of leukocytes adhesion, expression of cell adhesion molecules (CAMs) and MCP-1, IL-8, and activation of NF-κB [18, 23–27]. In addition, HG causes endothelial cell dysfunction through the generation of free radicals and that reactive oxygen intermediates induce NF-κB activation [27–29]. Therefore, in this study, the effects of Asp and Not (Fig. 1), the two active dihydrochalcones, on high glucose (HG)-induced vascular inflammation were determined *in vitro* and *in vivo*.

Effects of Dihydrochalcones on HG-Induced Disruption of the Endothelial Barrier Function of HUVECs and in Mice

Previous evidence has suggested that endothelial dysfunction and damage are early steps in the pathophysiology of vascular complications in diabetes mellitus [30]. Hyperglycemia is the central initiating factor for all types of diabetic microvascular disease, and it may also be involved in the pathogenesis of macrovascular complications [30–32]. In addition, endothelial cell permeability is impaired in diabetes mellitus and may be increased by high concentrations of extracellular glucose [33]. Leakage of serum proteins, particularly albumin, through the endothelium is observed in retinal vessels early in diabetes mellitus [33, 34]. Increased endothelial cell permeability in larger vessels leads to development of interstitial edema and may
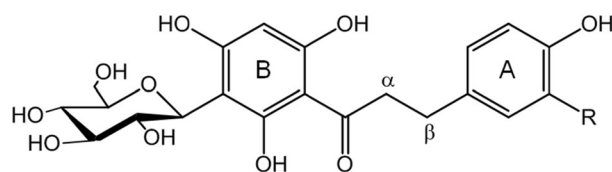
Dihydrochalones

Aspalathin (with *C*-*β*-D-glucopyranosyl): R = OH

Nothofagin (with *C*-*β*-D-glucopyranosyl): R = H

Fig. 1. Chemical structures of aspalathin (Asp) and nothofagin (Not).

result in enhancement of cell proliferation and matrix production [32]. Therefore, we first investigated the effects of glucose on the albumin permeability of endothelial cells, as shown in Fig. 2a. Treatment with HG (25 and 50 mM) led to a rapid increase in endothelial cell permeability (Fig. 2a). This effect began from 12 h after incubation and reached its maximum at 24 h (Fig. 2b). A significant increase was observed at a glucose concentration of 10 mM. Concentrations above 50 mM did not further increase the glucose-induced permeability (data not shown). L-Glucose and D-mannose (25 mM), which were used as an osmotic control, had no significant effect on endothelial cell permeability (Fig. 2a).

Next, we attempted to determine whether Asp or Not could alter HG-induced hyperpermeability. Treatment with 50 μM each compound alone did not result in alteration of

barrier integrity (Fig. 2c). As shown in Fig. 2c, treatment with Asp or Not resulted in a dose-dependent decrease in HG-mediated membrane disruption. To confirm this vascular-protective effect *in vivo*, HG-mediated vascular permeability in mice was assessed. As shown in Fig. 2d, treatment with Asp or Not resulted in markedly inhibited peritoneal leakage of dye induced by HG. Because the average weight of a mouse is 20 g and the average blood volume is 2 mL, the injected Asp (4.5, 9.1, 27.1, or 45.2 μg/mouse) or Not (4.4, 8.7, 26.2, or 43.6 μg/mouse) produced a concentration maximum of 5, 10, 30, or 50 μM in peripheral blood. To test the effects of cellular viability of Asp or Not, MTT assays were performed in HUVECs treated with each compound for 24 h. At the concentrations used (up to 50 μM), Asp or Not did not affect cell viability (Fig. 2e). These findings demonstrate inhibition of HG-
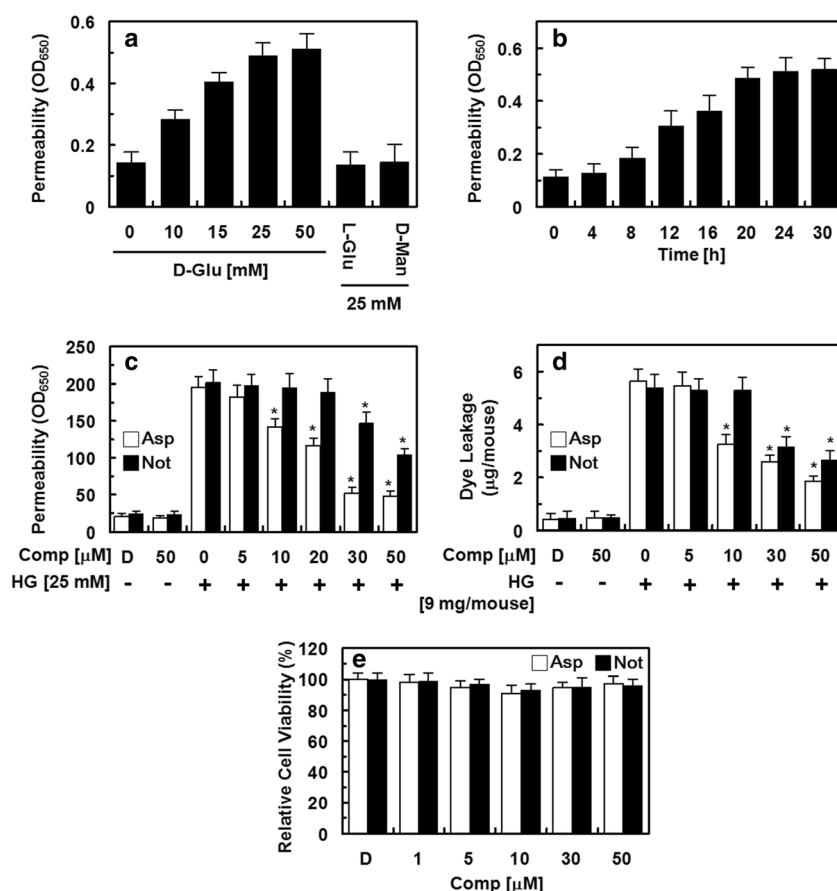

Fig. 2. Effects of Asp or Not on HG-mediated permeability *in vitro* and *in vivo*. **a** HUVECs were treated with D-glucose (0–50 mM), L-glucose (25 mM), or D-mannitol (25 mM) for 24 h and permeability was monitored. **b** HUVECs were treated with D-glucose (25 mM) for indicated time periods and permeability was monitored. **c** The effects of pretreatment with different concentrations of Asp (*white bar*) or Not (*black bar*) for 6 h on barrier disruptions caused by treatment with 25 mmHg for 24 h. **d** The effects of Asp (*white bar*) or Not (*black bar*) injected intravenously on HG-induced (9 mg/mouse, i.v.) vascular permeability in mice were determined (expressed μg/mouse, $n=5$). **e** The effects of Asp (*white bar*) or Not (*black bar*) on cell viability were measured using MTT assays. Results are expressed as the mean±SEM of at least three independent experiments. *$p<0.05$ *versus* HG alone (**c**, **d**).

mediated endothelial disruption and maintenance of human endothelial cell barrier integrity by Asp or Not in mice treated with HG. Therefore, prevention of HG-induced release of HMGB1 by each compound suggests the potential of Asp or Not in treatment of vascular inflammatory diseases.

Effects of Dihydrochalcones on HG-Mediated Expression of CAMs and THP-1 Adhesion

Two key early events in pathogenesis of atherosclerosis are adhesion of monocytes to the endothelium followed by transmigration into the subendothelial space and enhanced vascular cellular permeability [33, 35]. Increased leukocyte-endothelial interactions with monocytes from *in vivo* and *in vitro* diabetes models have been demonstrated [35, 36]. Of particular importance, the hyperglycemia/high glucose-induced augmentation of leukocyte adhesion to the endothelium through upregulation of cell surface expression of CAMs and transendothelial migration (TEM) has been reported to be dependent on NF-κB activation [27, 37]. In addition, CAMs are believed to participate in the pathogenesis of atherosclerosis [38]. These proteins regulate interaction between endothelium and leukocytes, and an increase in their expression on the endothelial surface causes increased adhesion of leukocytes, particularly monocytes, which are well known as one of the first steps in the process leading to atheroma [38]. In particular, over-expression of VCAM-1, ICAM-1, and E-selectin in endothelial cells in human

atherosclerotic lesions has been reported [39]. The effects of high glucose concentrations on expression of CAMs in endothelial cells have been widely investigated. The increase of ICAM-1 has been reported in human aortic endothelial cells cultured in high glucose [40]; these data are consistent with findings indicating that high glucose is a potent promoter of leukocyte adhesion to endothelial cells under flow conditions, depending on upregulation of E-selectin, ICAM-1, and VCAM-1 [27]. Furthermore, one of the earliest events in the vascular inflammation process is adhesion of monocytes to the endothelium, which is followed by their infiltration and differentiation into macrophages [41]. This key step is mediated by an interaction between monocytes and molecules expressed on the surface of endothelial cells [41]. These CAMs primarily mediated the adhesion of monocytes specifically found in atherosclerosis lesions of the vascular endothelium [41]. Therefore, we determined the effects of HG on expression of CAMs and adhesion of monocytes to HUVECs in response to HG. The responses according to concentration of HG in expression of CAMs, such as VCAM-1, ICAM-1, and E-selectin, were determined by cell ELISA. Exposure of the primary cultured HUVECs to HG resulted in significantly increased expression of VCAM-1, ICAM-1, and E-selectin after incubation with 25 mM D-glucose; the maximum inhibitory effect of Asp or Not (Fig. 3a) was observed at 50 μM.

In addition, in order to explore the effect of Asp or Not on endothelial cell–leukocyte interaction, we examined adhesion of THP-1 cells to high glucose-activated HUVECs.
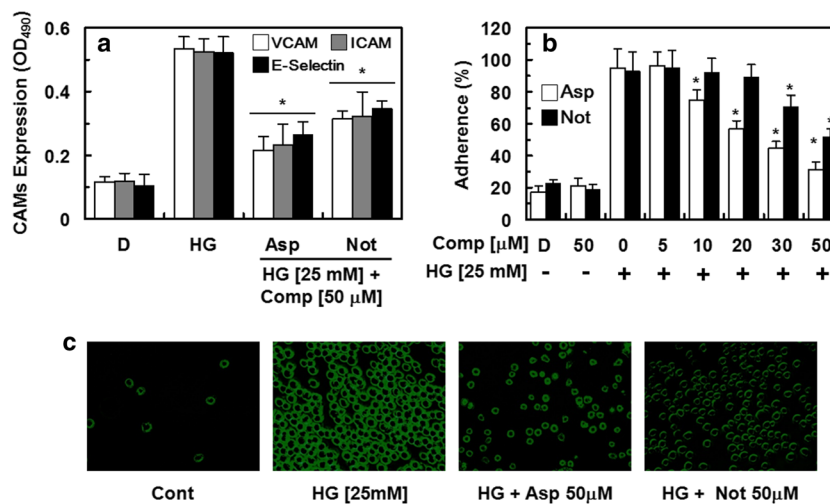

Fig. 3. Effects of Asp or Not on HG-mediated pro-inflammatory responses. **a** HG-induced (25 mM, for 24 h) expression of CAMs in HUVECs was determined after treatment of cells with Asp (50 μM, *white bar*) or Not (50 μM, *black bar*) for 6 h. VCAM-1 (*white bar*), ICAM-1 (*gray bar*), and E-selectin (*black bar*) were detected by ELISA. **b, c** HG-induced (25 mM, for 24 h)-mediated adherence of monocytes to HUVEC monolayers was assessed after pretreatment of cells with Asp (*white bar*) or Not (*black bar*) for 6 h. The amounts of adherent THP-1 cells were monitored by **b** cell–cell adhesion assay and **c** fluorescence microscopy. Data are expressed as the mean±SEM of three independent experiments. *p<0.05 and *p<0.05 *vs.* HG alone.
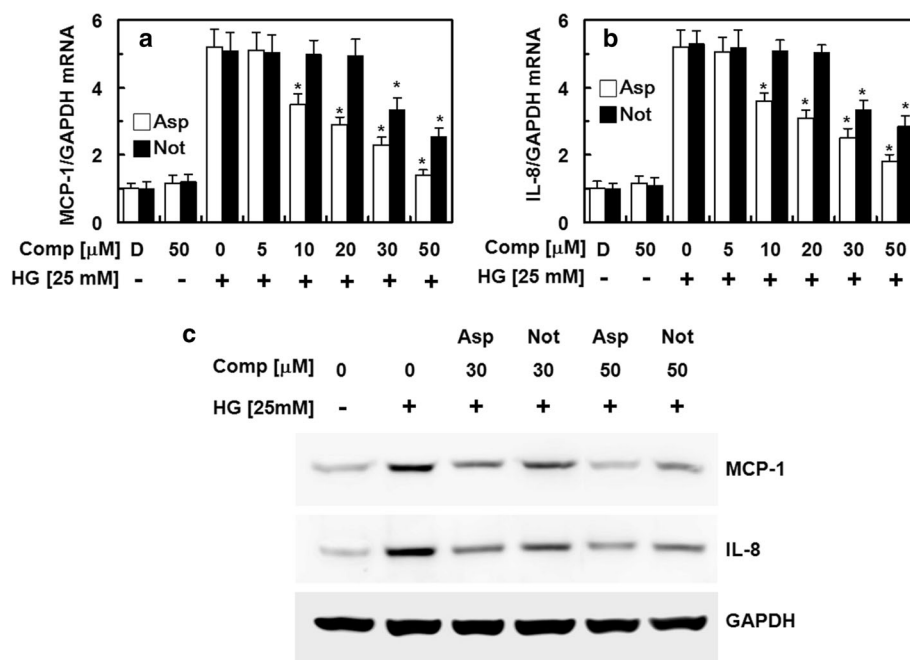
Fig. 4. Effects of Asp or Not on HG-induced mRNA and protein expressions of MCP-1 and IL-8 in HUVECs. Cells were pretreated with indicated concentrations of Asp (*white bar*) or Not (*black bar*) for 6 h and then incubated with HG (25 mM) for 48 h. Real-time qRT-PCR analysis was performed using specific primers for MCP-1, IL-8, and GAPDH, as described in "Materials and Methods." Data are expressed as the mean±SEM of three independent experiments. *$p < 0.05$ *vs.* HG alone. **c** Western blotting for MCP-1 and IL-8. GAPDH was used as an intra-control.

Control HUVECs showed minimal binding to THP-1 cells; however, adhesion showed a marked increase upon treatment with HG. Pretreatment with Asp or Not (50 μM) resulted in a decrease in the number of THP-1 cells adhering to HG-induced HUVECs (Fig. 3b, c). Thus, Asp or Not could be used as a therapeutic drug candidate for diabetic vascular inflammation targeting CAMs expression in prevention of atherosclerotic lesions.

MCP-1 and IL-8 are the chemokines most strongly implicated in the atherogenesis process [42]. MCP-1 is a key mediator of monocyte trafficking and IL-8 is chemotactic for neutrophils [42]. Thus, we measured the effect of Asp or Not on HG-induced MCP-1 and IL-8 mRNA levels using real-time qRT-PCR. As shown in Fig. 4a, b, HG induced an increase in expression levels of MCP-1 (up to 5.2-fold) and IL-8 (up to 5.1-fold) mRNA and pretreatment with Asp or Not resulted in decreased expression levels of HG-induced MCP-1 and IL-8 mRNA. The effects of Asp or Not on HG-induced MCP-1 and IL-8 protein levels were confirmed by Western blotting analysis (Fig. 4c). These results suggested that Asp or Not may be useful in prevention of the vascular inflammatory process.

Effect of Dihydrochalcones on HG-Induced Oxidative Stress

Inflammatory responses have been mechanistically linked to production of reactive oxygen species (ROS) [43]. Previous observations have indicated that hyperglycemia triggers generation of free radicals, and oxidant
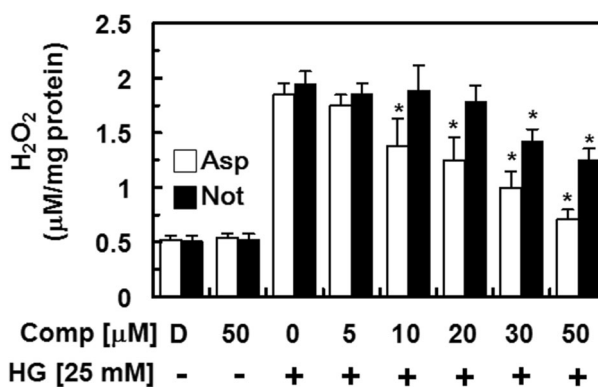

Fig. 5. Effects of Asp or Not on HG-induced ROS formation. Cells were pretreated with Asp (*white bar*) or Not (*black bar*) for 6 h and then stimulated with HG for 1 h. H_2O_2 assay were performed as described in the "Materials and Methods." Data are expressed as the mean±SEM of three independent experiments. *$p < 0.05$ *vs.* HG alone.

stress in various cell types and ROS are considered to be important mediators of several biologic responses, including cell proliferation, and extracellular matrix deposition [44, 45]. Therefore, to examine the protective effect of Asp or Not in HG-induced oxidative stress, we measured the effect of HG on cellular H_2O_2 concentration. The H_2O_2 level showed a statistically significant increase after incubation for 10 min with 25 mM glucose, and a maximal

increase was observed at 1 h (data not shown). Thus, we chose to determine cellular reactive oxygen species (ROS) at 1 h after glucose treatment in subsequent experiments. As shown in Fig. 5, pretreatment with Asp or Not resulted in significantly inhibited HG-induced H_2O_2 level. In addition, Asp or Not itself did not induce oxidative stress (data not shown), which suggested the importance of high glucose-induced oxidative stress from HUVECs in
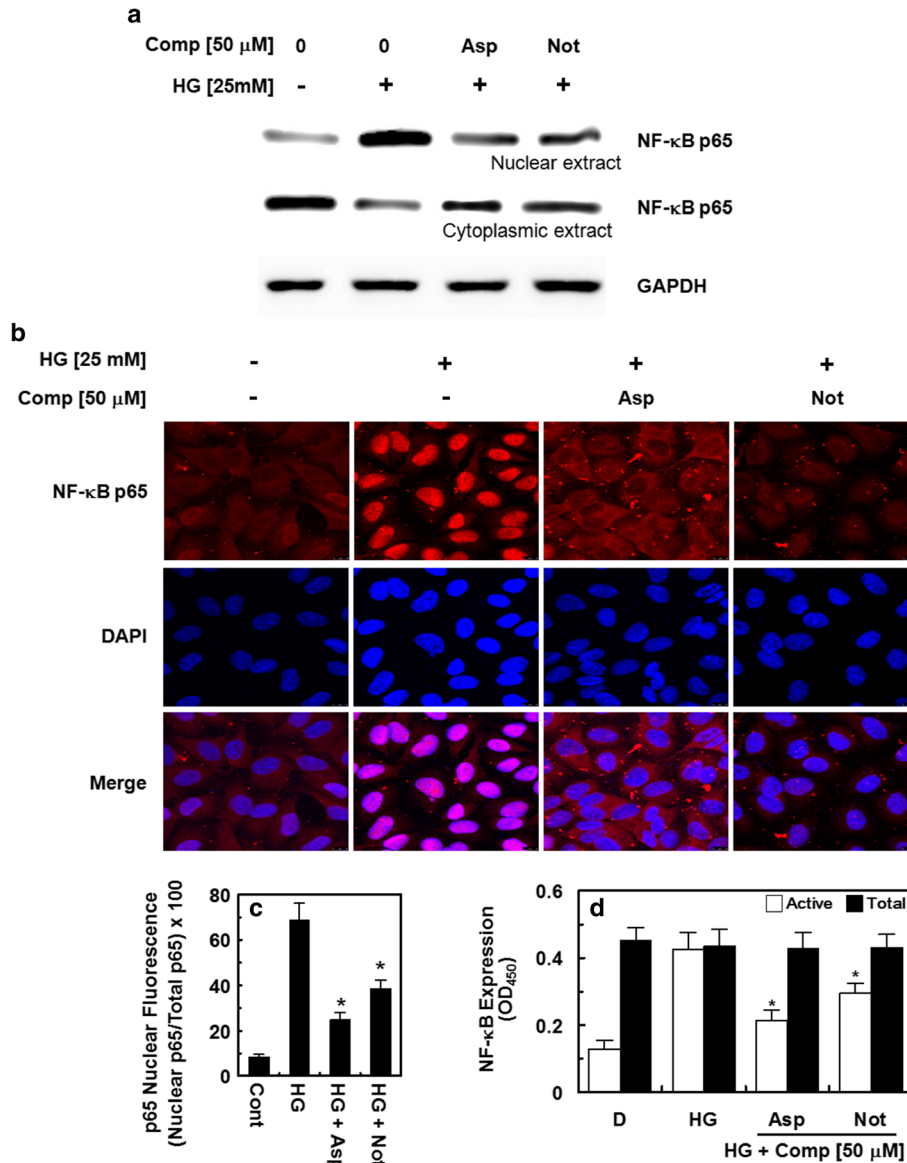

Fig. 6. Effects of Asp or Not on HG-induced activation of NF-κB. **a** Cells were pretreated with Asp or Not (50 μM) for 6 h and then stimulated with HG for 1 h. **b** NF-κB p65 was visualized using rabbit anti-p65 monoclonal antibody (1:100), which specifically recognizes NF-κB p65. The images are representative of results from three independent experiments. The quantification of p65 nuclear translocation is shown in **c**. **d** Cells were pretreated with Asp or Not (50 μM) for 6 h and then stimulated with HG (25 mM) for 1 h. HG-mediated expression of phospho-NF-κB p65 (*white bar*) or total NF-κB p65 (*black bar*) in HUVECs was analyzed by ELISA as described in the "Materials and Methods." *$p<0.05$ vs. HG alone.

determining the character of diabetic complication as well as vascular inflammation.

Effect of Dihydrochalcones on HG-Induced Activation of NF-κB

Activation of transcription factors such as NF-κB is known to affect CAMs and to induce a coordinated upregulation of other pro-inflammatory cytokines and chemoattractants, which possibly provide the molecular link between cell redox state and endothelial cell dysfunction [46]. In addition, ROS has been shown to activate various transcription factors, including NF-κB in cultured endothelial cells [47]. First, we measured HG-induced translocation of NF-κB from cytosol to nucleus. In Western blotting analysis for determination of NF-κB p65 protein level, the active subunit of the NF-κB complex, an increase in the level of the p65 protein was observed in the nuclear extracts of HUVECs treated with HG and the cytosolic extracts exhibited an appreciable loss of p65 protein content (Fig. 6a). In addition, pretreatment with Asp or Not resulted in inhibition of the HG-induced increase of p65 NF-κB expression levels (Fig. 6a). To confirm consistency with the result of Western blotting, immunocytochemistry was performed using p65 NF-κB and fluorescein isothiocyanate (FITC)-conjugated antibody. As a result, HG induced an increase in expression of p65 NF-κB in the nucleus, whereas normal condition did not (Fig. 6b, c). In addition, treatment with 50 μM Asp or Not resulted in a decrease in HG-induced expression of p65 NF-κB in the nucleus (Fig. 6b, c). We also determined the effects of Asp or Not on the expressions of p65 NF-κB by ELISA, and data showed that treatment with HG resulted in increased expressions of NF-κB and these increases were significantly reduced by treatment with Asp or Not (Fig. 6d). These results were consistent with those of Western blotting (Fig. 6a), demonstrating that HG-induced activation of NF-κB was inhibited by Asp or Not, indicating that Asp or Not has some inhibitory effect on the NF-κB pathways specific to HG-induced adhesion molecules in HUVECs.

Previously, the OH groups located at C2′ and C6′ as well as the tautomerization of the keto–enol tautomerism of the carbonyl and α-methylene groups are believed to play important roles in the biological activity of dihydrochalcones [48, 49]. Therefore, suppression of HG-mediated inflammatory responses by Asp and Not provides a therapeutic strategy for management of sepsis and septic shock. However, between Asp and Not, the inhibitory effects of Asp on HG-induced signaling pathway were better than those of Not. A possible explanation for our results lies in the fact of the obvious difference between Asp and Not, the presence of the catechol-type A ring of Asp (Fig. 1). Therefore, the presence of a 3-OH in the A-ring contributes to the inhibitory effects of Asp in HG-induced signaling pathway. This concept could be explained by the previous findings which demonstrated that Not had slightly less potent antioxidant activity in an aqueous environment compared to Asp when using *in vitro* radical scavenging assays [50, 51]. Furthermore, Not exhibits a far less protecting effect against Fe(II)-induced lipid peroxidation in a lipid environment compared to Asp when using a hydrophobic biomembrane assay system [51]. Conformational differences and the absence of the catechol moiety in the Not molecular structure were postulated to explain differences in their antioxidant effects in hydrophobic/hydrophilic environments [51].

In summary, our results demonstrate that treatment with Asp and Not resulted in blockade of HG-induced vascular inflammation *via* inhibition of NF-κB in primary human endothelial cells. These results suggest that Asp and Not have significant therapeutic benefits against diabetic complications and atherosclerosis by attenuating HG-induced generation of H_2O_2, increased activation of NF-κB, upregulation of adhesion molecules, monocyte–endothelial adhesion, and disruption of the endothelial barrier function. Our findings indicate that Asp and Not can be regarded as candidates for use in treatment of diabetic vascular inflammatory diseases.

Conflict of Interest. None declared.

REFERENCES

1. Whiting, D.R., L. Guariguata, C. Weil, and J. Shaw. 2011. IDF diabetes atlas: global estimates of the prevalence of diabetes for 2011 and 2030. *Diabetes Research and Clinical Practice* 94: 311–321.
2. Grundy, S.M., I.J. Benjamin, G.L. Burke, *et al.* 1999. Diabetes and cardiovascular disease: a statement for healthcare professionals from the American Heart Association. *Circulation* 100: 1134–1146.
3. Thomas, J.E., and J.M. Foody. 2007. The pathophysiology of cardiovascular disease in diabetes mellitus and the future of therapy. *Journal of the Cardiometabolic Syndrome* 2: 108–113.

4. Roglic, G., N. Unwin, P.H. Bennett, *et al*. 2005. The burden of mortality attributable to diabetes: realistic estimates for the year 2000. *Diabetes Care* 28: 2130–2135.

5. Rubino, F., and M. Gagner. 2002. Potential of surgery for curing type 2 diabetes mellitus. *Annals of Surgery* 236: 554–559.

6. Day, C. 1998. Traditional plant treatments for diabetes mellitus: pharmaceutical foods. *British Journal of Nutrition* 80: 5–6.

7. Li, G.Q., A. Kam, K.H. Wong, *et al*. 2012. Herbal medicines for the management of diabetes. *Advances in Experimental Medicine and Biology* 771: 396–413.

8. Prior, R.L., and G. Cao. 1999. Antioxidant capacity and polyphenolic components of teas: implications for altering *in vivo* antioxidant status. *Proceedings of the Society for Experimental Biology and Medicine* 220: 255–261.

9. Warren, C.P. 1999. Antioxidant effects of herbs. *Lancet* 353: 676.

10. McKay, D.L., and J.B. Blumberg. 2007. A review of the bioactivity of South African herbal teas: rooibos (Aspalathus linearis) and honeybush (Cyclopia intermedia). *Phytotherapy Research* 21: 1–16.

11. Kazuno, S., M. Yanagida, N. Shindo, and K. Murayama. 2005. Mass spectrometric identification and quantification of glycosyl flavonoids, including dihydrochalcones with neutral loss scan mode. *Analytical Biochemistry* 347: 182–192.

12. Lee, W., S.K. Ku, and J.S. Bae. 2013. Emodin-6-O-beta-D-glucoside down-regulates endothelial protein C receptor shedding. *Archives of Pharmacal Research* 36: 1160–1165.

13. Bae, J.S., and A.R. Rezaie. 2013. Thrombin inhibits HMGB1-mediated proinflammatory signaling responses when endothelial protein C receptor is occupied by its natural ligand. *BMB Reports* 46: 544–549.

14. Kim, T.H., S.K. Ku, I.C. Lee, and J.S. Bae. 2012. Anti-inflammatory functions of purpurogallin in LPS-activated human endothelial cells. *BMB Reports* 45: 200–205.

15. Bae, J.S., W. Lee, and A.R. Rezaie. 2012. Polyphosphate elicits proinflammatory responses that are counteracted by activated protein C in both cellular and animal models. *Journal of Thrombosis and Haemostasis* 10: 1145–1151.

16. Lee, J.D., J.E. Huh, G. Jeon, *et al*. 2009. Flavonol-rich RVHxR from Rhus verniciflua Stokes and its major compound fisetin inhibits inflammation-related cytokines and angiogenic factor in rheumatoid arthritic fibroblast-like synovial cells and *in vivo* models. *International Immunopharmacology* 9: 268–276.

17. Bae, J.S., W. Lee, J.O. Nam, J.E. Kim, S.W. Kim, and I.S. Kim. 2014. Transforming growth factor beta-induced protein promotes severe vascular inflammatory responses. *American Journal of Respiratory and Critical Care Medicine* 189: 779–786.

18. Lee, W., S.K. Ku, D. Lee, T. Lee, and J.S. Bae. 2014. Emodin-6-O-beta-D–glucoside inhibits high-glucose-induced vascular inflammation. *Inflammation* 37: 306–313.

19. Mackman, N., K. Brand, and T.S. Edgington. 1991. Lipopolysaccharide-mediated transcriptional activation of the human tissue factor gene in THP-1 monocytic cells requires both activator protein 1 and nuclear factor kappa B binding sites. *Journal of Experimental Medicine* 174: 1517–1526.

20. Fuseler, J.W., D.M. Merrill, J.A. Rogers, M.B. Grisham, and R.E. Wolf. 2006. Analysis and quantitation of NF-kappaB nuclear translocation in tumor necrosis factor alpha (TNF-alpha) activated vascular endothelial cells. *Microscopy and Microanalysis* 12: 269–276.

21. Lee, W., S.K. Ku, and J.S. Bae. 2014. Vascular barrier protective effects of orientin and isoorientin in LPS-induced inflammation *in vitro* and *in vivo*. *Vascular Pharmacology* 62: 3–14.

22. Joubert, E., W.C. Gelderblom, A. Louw, and D. de Beer. 2008. South African herbal teas: aspalathus linearis, Cyclopia spp. and Athrixia phylicoides—a review. *Journal of Ethnopharmacology* 119: 376–412.

23. Ku, S.K., S. Kwak, and J.S. Bae. 2014. Orientin inhibits high glucose-induced vascular inflammation *in vitro* and *in vivo*. *Inflammation*. (in press).

24. Kim, J.A., J.A. Berliner, R.D. Natarajan, and J.L. Nadler. 1994. Evidence that glucose increases monocyte binding to human aortic endothelial cells. *Diabetes* 43: 1103–1107.

25. Lee, Y.J., D.G. Kang, J.S. Kim, and H.S. Lee. 2008. Lycopus lucidus inhibits high glucose-induced vascular inflammation in human umbilical vein endothelial cells. *Vascular Pharmacology* 48: 38–46.

26. Takaishi, H., T. Taniguchi, A. Takahashi, Y. Ishikawa, and M. Yokoyama. 2003. High glucose accelerates MCP-1 production via p38 MAPK in vascular endothelial cells. *Biochemical and Biophysical Research Communications* 305: 122–128.

27. Morigi, M., S. Angioletti, B. Imberti, *et al*. 1998. Leukocyte-endothelial interaction is augmented by high glucose concentrations and hyperglycemia in a NF-kB-dependent fashion. *Journal of Clinical Investigation* 101: 1905–1915.

28. Kashiwagi, A., T. Asahina, Y. Nishio, *et al*. 1996. Glycation, oxidative stress, and scavenger activity: glucose metabolism and radical scavenger dysfunction in endothelial cells. *Diabetes* 45(Suppl 3): S84–S86.

29. Du, X., K. Stocklauser-Farber, and P. Rosen. 1999. Generation of reactive oxygen intermediates, activation of NF-kappaB, and induction of apoptosis in human endothelial cells by glucose: role of nitric oxide synthase? *Free Radical Biology and Medicine* 27: 752–763.

30. Laakso, M. 1999. Hyperglycemia and cardiovascular disease in type 2 diabetes. *Diabetes* 48: 937–942.

31. Kannel, W.B., and D.L. McGee. 1979. Diabetes and cardiovascular disease. The Framingham study. *JAMA* 241: 2035–2038.

32. Nannipieri, M., L. Rizzo, A. Rapuano, A. Pilo, G. Penno, and R. Navalesi. 1995. Increased transcapillary escape rate of albumin in microalbuminuric type II diabetic patients. *Diabetes Care* 18: 1–9.

33. Wardle, E.N. 1994. Vascular permeability in diabetics and implications for therapy. *Diabetes Research and Clinical Practice* 23: 135–139.

34. Tooke, J.E. 1995. Microvascular function in human diabetes. A physiological perspective. *Diabetes* 44: 721–726.

35. Gerrity, R.G. 1981. The role of the monocyte in atherogenesis: I. Transition of blood-borne monocytes into foam cells in fatty lesions. *American Journal of Pathology* 103: 181–190.

36. Esposito, C., G. Fasoli, A.R. Plati, *et al*. 2001. Long-term exposure to high glucose up-regulates VCAM-induced endothelial cell adhesiveness to PBMC. *Kidney International* 59: 1842–1849.

37. Hamuro, M., J. Polan, M. Natarajan, and S. Mohan. 2002. High glucose induced nuclear factor kappa B mediated inhibition of endothelial cell migration. *Atherosclerosis* 162: 277–287.

38. Lopes-Virella, M.F., and G. Virella. 1992. Immune mechanisms of atherosclerosis in diabetes mellitus. *Diabetes* 41(Suppl 2): 86–91.

39. Bae, J.S. 2012. Role of high mobility group box 1 in inflammatory disease: focus on sepsis. *Archives of Pharmacal Research* 35: 1511–1523.

40. Kado, S., T. Wakatsuki, M. Yamamoto, and N. Nagata. 2001. Expression of intercellular adhesion molecule-1 induced by high glucose concentrations in human aortic endothelial cells. *Life Sciences* 68: 727–737.

41. Hansson, G.K., and P. Libby. 2006. The immune response in atherosclerosis: a double-edged sword. *Nature Reviews Immunology* 6: 508–519.

42. Boisvert, W.A. 2004. Modulation of atherogenesis by chemokines. *Trends in Cardiovascular Medicine* 14: 161–165.

43. Inoguchi, T., P. Li, F. Umeda, *et al*. 2000. High glucose level and free fatty acid stimulate reactive oxygen species production through protein kinase C-dependent activation of NAD(P)H oxidase in cultured vascular cells. *Diabetes* 49: 1939–1945.

44. Dunlop, M. 2000. Aldose reductase and the role of the polyol pathway in diabetic nephropathy. *Kidney International. Supplement* 77: S3–S12.

45. Han, H.J., Y.J. Lee, S.H. Park, J.H. Lee, and M. Taub. 2005. High glucose-induced oxidative stress inhibits Na+/glucose cotransporter activity in renal proximal tubule cells. *American Journal of Physiology. Renal Physiology* 288: F988–F996.

46. Rimbach, G., G. Valacchi, R. Canali, and F. Virgili. 2000. Macrophages stimulated with IFN-gamma activate NF-kappa B and induce MCP-1 gene expression in primary human endothelial cells. *Molecular Cell Biology Research Communications* 3: 238–242.

47. Uemura, S., H. Matsushita, W. Li, *et al*. 2001. Diabetes mellitus enhances vascular matrix metalloproteinase activity: role of oxidative stress. *Circulation Research* 88: 1291–1298.

48. Nakamura, Y., S. Watanabe, N. Miyake, H. Kohno, and T. Osawa. 2003. Dihydrochalcones: evaluation as novel radical scavenging antioxidants. *Journal of Agricultural and Food Chemistry* 51: 3309–3312.

49. Rezk, B.M., G.R. Haenen, W.J. van der Vijgh, and A. Bast. 2002. The antioxidant activity of phloretin: the disclosure of a new antioxidant pharmacophore in flavonoids. *Biochemical and Biophysical Research Communications* 295: 9–13.

50. Krafczyk, N., F. Woyand, and M.A. Glomb. 2009. Structure-antioxidant relationship of flavonoids from fermented rooibos. *Molecular Nutrition & Food Research* 53: 635–642.

51. Snijman, P.W., E. Joubert, D. Ferreira, *et al*. 2009. Antioxidant activity of the dihydrochalcones aspalathin and nothofagin and their corresponding flavones in relation to other rooibos (Aspalathus linearis) flavonoids, epigallocatechin gallate, and trolox. *Journal of Agricultural and Food Chemistry* 57: 6678–6684.